

Performance of the Transport Casks and Cladding Tubes for Fresh MOX fuel against External Water Pressure

Chihiro Itoh, Toshiari Saegusa

Central Research Institute of Electric Power Industry
Abiko Research Laboratory
1646 Abiko, Abiko-shi, Chiba-ken 270-1194 JAPAN

1. Introduction

In Japan, for the time being, up to commercial commissioning of fast breeder reactors, MOX fuel is planned to be utilized in light water reactors in Japan. The plutonium recovered in overseas reprocessing plant is basically used for fabrication of MOX fuel in Europe and MOX fuel is supposed to be transported to Japan by sea.

There is a special safety standard called the INF Code at IMO (International Maritime Organization) which pertains to the structure and systems of the sea transport ship. In Japan, the Director-General of the Maritime Technology and Safety Bureau, Ministry of Transport has founded a technical standard that reflects the INF Code. It is stipulated in these safety standards in addition to normal standards, that the ship has a securing system, automatic collision preventive system, etc. for the aspect of systems, and has a structure protected from collision, running aground, etc. for the structural aspect. Therefore, it is considered that there is little possibility of an abnormal accident such as a collision with another ship, sinking in the sea, etc.

The probability of the submergence of ships is found in the literature¹⁾²⁾. Sprung, et al.(1998), which estimated the probability of extremely severe accidents that a charter freighter might experience during a voyage from Charleston, South Carolina, directly to Cherbourg, France. Because the collision-only accident analyzed is the least severe accident expected to cause package failure, while the double failure, collision-plus-fire accident, is probably about as severe an accident as is at all credible, the range of these results, 10^{-6} to 10^{-11} , represents the likely range for the release of radioactivity from a Type B spent fuel package during a transatlantic crossing. It should be noted that the Charter Freighter is classified as an INF-2 vessel under the INF Code. The INF-2 vessel may have a single-hull structure. On the other hand, the fresh MOX fuel will be transported to Japan by a vessel with a double-hull structure in accordance with the special regulation in Japan as mentioned above. Therefore, the possibility of accidental damage to the package is far less and the probability of the severe ship accident leading to the release of radioactivity from a Type B package is far less than the range of 10^{-6} to 10^{-11} /voyage. Watabe, et al. (1998) estimated that the probability of total-loss of an exclusive ship (double-hull structure) without accidental damage to a package shipping radioactive materials from Europe to Japan is 2.6×10^{-5} /voyage. The probability of submergence of ships, therefore, is considered to be less than 2.6×10^{-5} /voyage.

2. Purpose

The purpose of this study is to evaluate the performance of transport casks and claddings for fresh MOX fuel against external water pressure. Despite the improbability of extremely severe ship accidents, it is important to evaluate the ability of transport casks and fuel claddings for fresh MOX fuel to withstand external water pressure when they were hypothetically submerged into the sea for unexpected reasons.

3. Performance of the Transport Cask for Fresh MOX fuel against External Water Pressure

3.1 Outline of the Casks

The analyses were carried out for TN-12B(M) and EXL-4(M) (here- after called the TN cask and the EXL cask) which will be used to transport fresh MOX fuels from Europe to Japan. These casks have been already assessed to withstand external pressure of 200m under water (the IAEA Regulation for the Safe Transport of Radioactive Materials,1996 Edition, No.ST-1) . Also, it is considered these casks will withstand more external water pressure because the thickness of the body and lid of the cask are decided based on shielding protection and have usually rather a large thickness for external water pressure.

3.2. Analytical Condition

Analytical Code

ABAQUS, the general-purpose non-linear code with a finite element method is used for the analysis.

Analytical Model

Finite element models of the TN cask and the EXL cask are shown in Fig.1 and Fig.2, respectively. The basket, neutron shielding material, heat transfer fins and shock absorber in the casks that do not have any effect on the ability of the casks to withstand external water pressure are not considered in the analysis. The axis-symmetric solid element is adopted to model the casks.

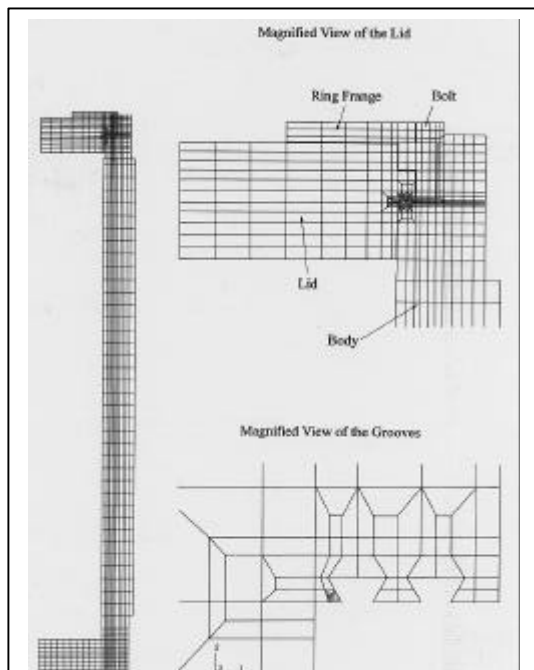


Fig.1 Finite Element Model -TN Cask-

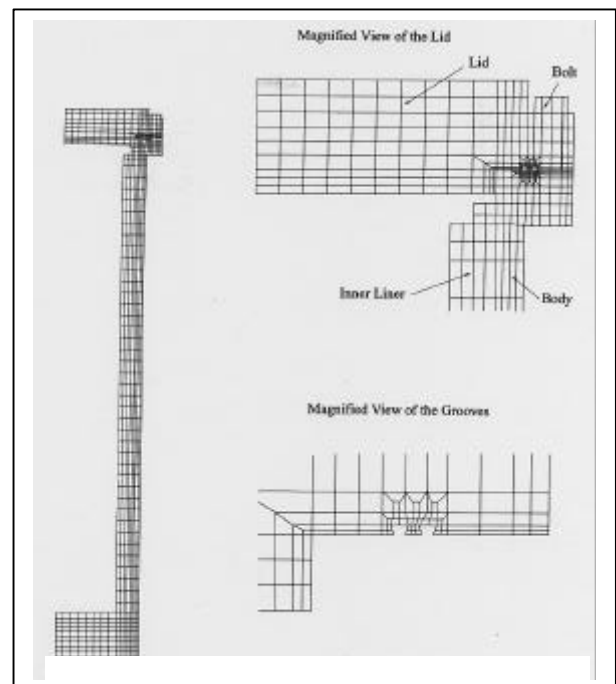


Fig.2 Finite Element Model -EXL Cask-

The

- Lid bolts are modeled using an axis-symmetric ring which has the same thickness with the diameter of the bolt hole at the lid.
- Inner pressure in the cask cavity is not considered because it is much lower than the external water pressure.
- Interface elements are applied to the contact surface between lid and body. These elements can allow the simulation of the behavior of the lid.
- External water pressure is applied to the cask model as an external uniformly distributed load.
- Initial bolting load is considered as a pre-stress of the element for the bolts.

Failure Criterion

The failure criterion of casks against external water pressure is defined as the maximum water depth at which structural parts such as the cask body and lid do not rupture. Based on the CRIEPI's way of thinking, the failure criterion could be indicated when the Von-Mises stress exceeds the ultimate tensile strength at the structural parts of casks in the analytical evaluation.

3.4 Results

TN Casks

Stress distributions over the body and lid are shown in Figs. 3 and 4, respectively. As indicated in Fig. 3, no stress exceeds the tensile ultimate strength even under 11,000m of water. The cask body will not rupture under such a depth of water. The stress exceeds the ultimate tensile strength at a part of the base of the lid flange under 7,000m of water as shown in Fig. 4.

Analytical results focusing on a stress state related to containment in the vicinity of the O-ring gasket attached to the lid are shown in Fig. 5. The stress exceeds the ultimate tensile strength at the part between the grooves for the O-ring gaskets under 4,000m of water as shown in Fig. 5. However, the lid does not open because compressive stress is acting over the contact zone between the lid and cask body under a water depth of 4,000m and even 7,000m as illustrated in Fig. 6. From these results, leak tightness is considered to be kept actually under a further depth of water..

EXL Cask

Stress distributions over the body and lid are shown in Figs. 7 and 8, respectively.

As indicated in Fig. 7, the stress exceeds the ultimate tensile strength at the upper part of the cask body under a water depth of 9,600m. The stress exceeds the ultimate tensile strength at a part of the base of the lid flange under a water depth of 10,000m as shown in Fig.8.

Analytical results focusing on the stress state related to containment in the vicinity of the O-ring gasket attached to the lid are shown in Fig. 9. The stress exceeds the ultimate tensile strength at the part between the grooves for the O-ring gaskets under a depth of 7,600m as shown in Fig. 9. However, the lid does not open because compressive stress is acting over the contact zone between the lid and cask body under a water depth of 7,600 and even 10,000m as illustrated in Fig. 10. From these results, leak tightness is considered to be kept actually under a further depth of water.

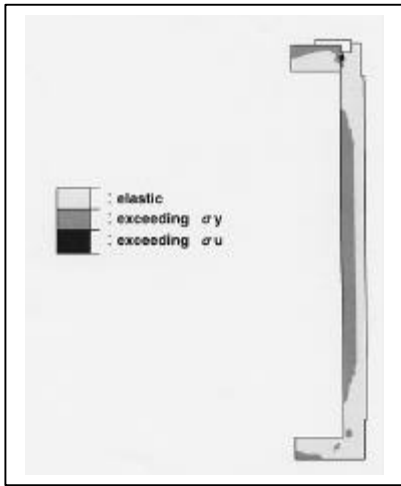


Fig.3 Stress Distribution in the Body of TN Cask
–Mises Stress- (11,000m depth)

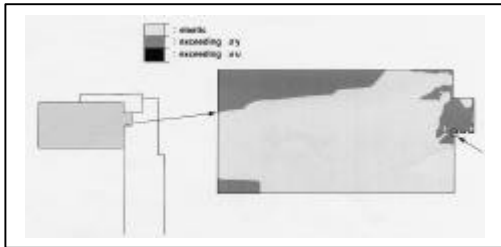


Fig.4 Stress Distribution in the Lid of TN Cask
–Mises Stress- (7,000m depth)

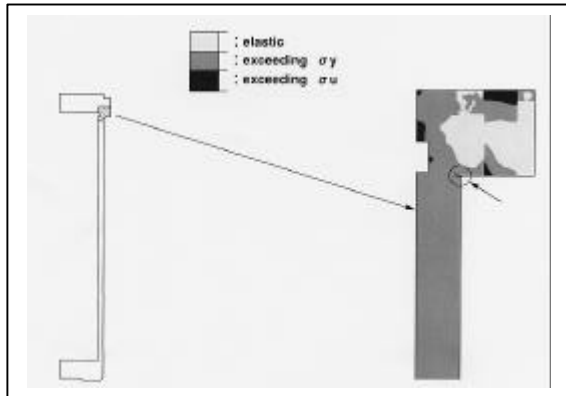


Fig.7 Stress Distribution in the Body of EXL Cask
–Mises Stress- (9,600m depth)

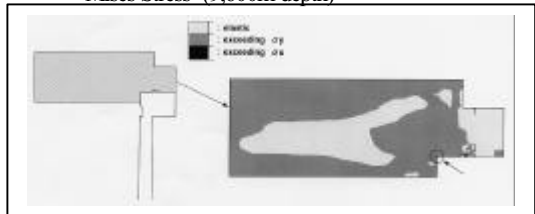


Fig.8 Stress Distribution in the Lid of EXL Cask
–Mises Stress- (10,000m depth)

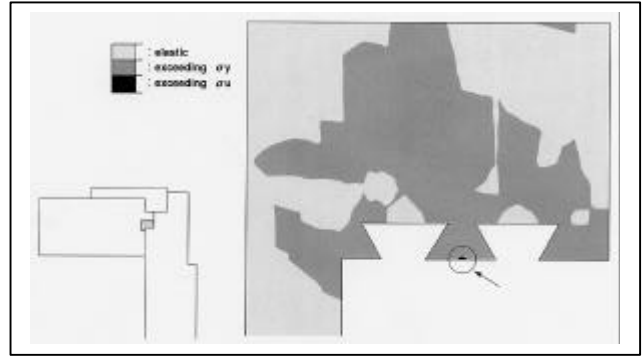


Fig.5 Stress Distribution in the Vicinity of Grooves for O-ring
Gasket of TN Cask –Mises Stress- (4,000m depth)

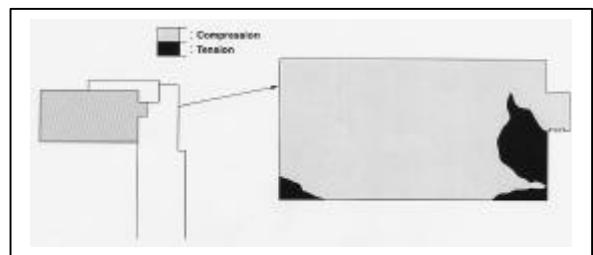


Fig.6 Axial Compression Stress Distribution in the Lid of TN
Cask (7,000m depth)

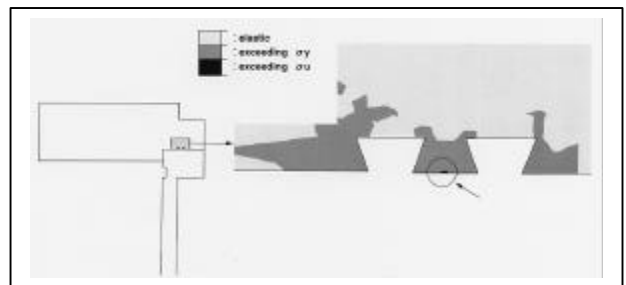


Fig.9 Stress Distribution in the Vicinity of Grooves for O-ring
Gasket of EXL Cask –Mises Stress- (7,600m depth)

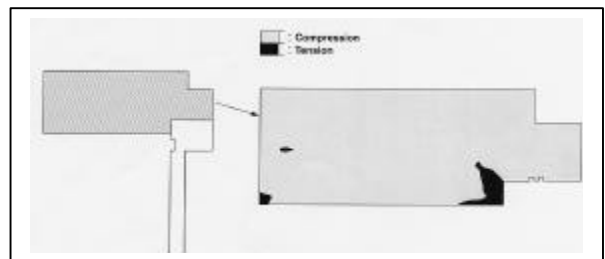


Fig.10 Axial Compression Stress Distribution in the Lid of
EXL Cask (10,000m depth)

4. Performance of the Claddings Tube against External Water Pressure

4.1 Test Specimens and Conditions

Outlines of the specimens are shown in Fig. 11. The specimens have the following characteristics.

- Cladding tubes have the same dimensions (inner and outer diameter:10.6mm/12.3mm for BWR-type, 8.36mm/9.5mm for PWR-type) as the real ones except for their length. The length of the test specimens is made shorter to the extent (BWR type: 1,100mm, PWR type:700mm) that the behavior of the specimens against external pressure does not change based on the preliminary evaluation.
- Aluminum ceramic is adopted as a material for simulated fuel pellets in consideration of its mechanical properties. However, the mechanical properties of the fuel pellets are considered to have little effect on the behavior of the cladding tube and the outcome of the test because an preliminary evaluation conducted in advance of the tests showed the stress in the fuel pellets is less than a yield stress.
- The materials of the cladding tubes (BWR type: zircaloy-2, PWR type: zircaloy-4) and the plugs are the same materials as the real ones.
- Real springs were used
- The method of welding is also same as the real one.

The test conditions are shown in Table1.

4.2 Test Results

BWR-type fuel cladding

A summary of the test result is shown in Table 2.

The typical stress-strain relationship under a pressure of up to 98MPa (approximately a depth of water of 10,000m) is illustrated in Fig.12. As shown in this figure, the relationship between the pressure and the strain is linear under a pressure of up to 69MPa (approximately a depth of water of 7,000m), then the strain increases rapidly due to rupture at around a pressure of 73MPa (approximately a depth of water of 7,400m). And, it can be seen that the axial strain increases smoothly from when the strain reached about 1.4%. A maximum measured strain is about 6% that is far less than the ultimate strain of 34% of this material. At the outer surface of the cladding tube of the plenum part, a wave - like surface appeared along with the shape of a spring located inside the tube and small cracks were observed on it. On the other hand, the cladding tube of the fuel part was slightly deformed elliptically but cracks were not observed.

In order to see the behavior of buckling of the cladding tubes in detail, pressure tests under a maximum pressure of 73MPa, 74MPa and 78MPa(approximately a depth of water of 7,400m, 7,500m and 8,000m) were carried out. The typical stress-strain curves measured in the tests in which the maximum pressures were 74MPa (approximately a depth of water of 7,400m~7,500m)are shown in Fig.13. Under a pressure of 69MPa~72MPa (approximately a depth of water of 7,000m~7,300m), the cladding tubes ruptured and the strains at the plenum part of the cladding tube increased rapidly without an increase of external pressure. The measured strain of 0.38% from which a rapid increase of strain starts is almost coincident with the yield strain 0.382%. Therefore, it is considered that the rupture could be due to a plastic flaw triggered by the occurrence of yield strain.

At the test under the maximum pressure of 73MPa (approximately a depth of water of 7,400m), only the cladding tube was deformed. The cladding tube of the fuel part was slightly deformed elliptically but crack were not observed. On the other hand, the spring inside the cladding tube was also deformed in a radial direction under a pressure of 74MPa (approximately a depth of water of 7,500m) and finally both the cladding tube and spring turned into an elliptical shape. A wave - like surface appeared at the outer surface of the cladding tube along with the shape of the spring located inside the tube and small cracks were observed on it.

Leak-tightness tests with the helium-leak method were carried out after the tests. The test results show that the leak tightness was kept with the specimens subjected to the tests under a maximum pressure of 2MPa(approximately a depth of water of 200m) and 73MPa (approximately a depth of water of 7,400m) in which

only the cladding tube ruptured. The specimens after the test under a maximum pressure of 73MPa (approximately a depth of water of 7,400m) are shown in Photo.1.

PWR type

A summary of the test result is shown in Table 3.

The typical stress-strain relationship under a pressure of up to 98MPa (approximately a depth of water of up to 10,000m) is illustrated in Fig.14. As shown in this figure, the relationship between the pressure and the strain is linear under a pressure of up to 49Mpa(approximately a depth of water of 5,000m), then the strain increases rapidly due to a rupture at around a pressure of 54MPa (approximately a depth of water of 5,500m) following that the strain grew with pressure. This is because the cladding tube was deformed, contacting the spring inside the tube, then the spring withstood the water pressure. A maximum measured strain is about 1.4% which is far less than the ultimate strain of 18% of this material. A wave-like pattern appeared slightly at the outer surface of the cladding tube along with the shape of the spring. However, cracks were not observed. On the other hand, the cladding tube of the fuel part was slightly deformed elliptically but cracks were not observed.

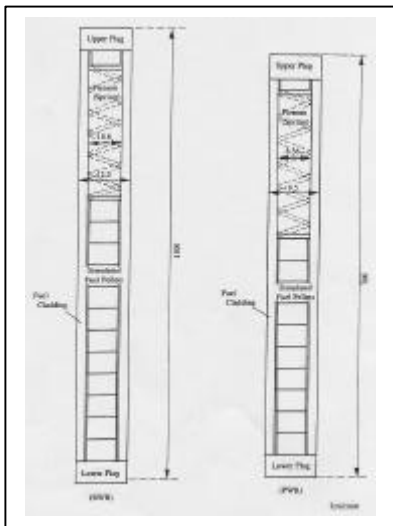


Fig.11 Fuel Cladding specimens

Table 1 Test Conditions

Type	Test No.	Number of Specimens	Max. Pressure (MPa)	Duration Time for Test (min.)
B W R	No.1	3	2	60
	2-1	3	73	5
	No.2-2	3	74	10
	2-3	3	78	20
	No.3	3	98	60
P W R	No.1	3	2	60
	2-1	3	59	5
	No.2-2	3	69	10
	2-3	3	88	20
	No.3	3	98	60

In order to see the behavior of a rupture of the cladding tubes in detail, pressure tests under maximum pressure of 59MPa, 69MPa and 88MPa (approximately a depth of water of 6,000m, 7,000m and 9,000m) were carried out. The typical stress-strain curves measured during the tests in which the maximum pressure was 69MPa are shown in Fig.15. Under a pressure of 59MPa (approximately a depth of water of 6,000m), the cladding tubes ruptured and the strains at the plenum part of the cladding tube increased rapidly. After an increase of strain of 0.400% due to buckling the strain grew with pressure as seen in 98MPa pressure test. As the measured strain 0.4% at which a rupture of the cladding tube occurred is smaller than yield strain 0.616%, it can be said that this rupture is considered to be an elastic buckling.

Leak-tightness tests with the helium-leak method were carried out after the tests and the test results show that leak tightness was kept at all specimens. The specimens after the test under a maximum pressure of 98MPa (approximately a depth of water of 10,000m) were shown in Photo.2

5. Conclusion

Structural analyses using finite element method and pressure tests were carried out to evaluate the ability of the transport casks and cladding tubes for fresh MOX fuel respectively against external water pressure.

The analytical results of the casks show that the TN cask and EXL cask will not rupture under a water depth of 7,000m.

The test results of the cladding tubes show that the cladding tubes for the BWR-type can resist until an external water pressure of 69MPa (approximately a depth of water of 7,000m) and that of PWR-type fuel can resist until an external water pressure of 54MPa (approximately a depth of water of 5,500m). Moreover, leak tightness is maintained at an external water pressure of 73MPa (approximately a depth of water of 7,400m) for the BWR-type cladding tubes and until an external water pressure of 98MPa (approximately a depth of water of 10,000m) for the PWR type cladding tubes.

Table 2 Summary of Test Results of BWR type Fuel Rod

Specimens	Pressure (MPa)	Buckling Pressure (MPa)		Crack
		Fuel cladding	Spring	
No.1	2	---	---	none
		---	---	
		---	---	
2-1	73	70	---	none
		69	---	
		70	---	
No.2-2	74	71	74	yes
		72	74	
		70	74	
2-3	78	71	76	yes
		72	75	
		70	76	
No.3	98	71	74	yes
		72	76	
		69	76	

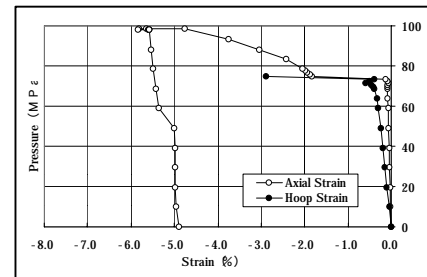


Fig.12 Test Result of BWR Cladding (98MPa)

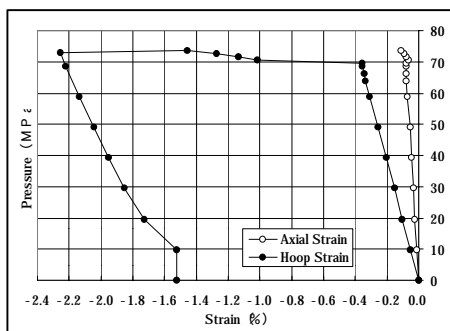


Fig.13 Test Result of BWR Cladding (74MPa)

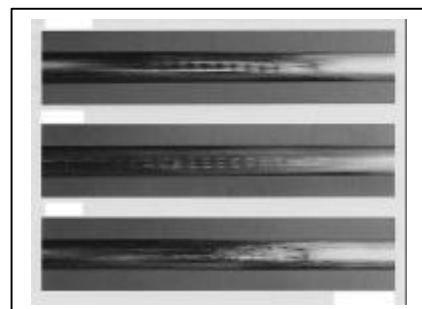


Photo.1 BWR Claddings after Buckling

Table 3 Summary of Test Results of PWR type Fuel Rod

Specimens		Pressure (MPa)	Buckling Pressure(MPa)		Crack
			Fuel cladding	Spring	
No.1	a	2	-----	-----	none
	b		-----	-----	
	c		-----	-----	
2-1	a	59	57	-----	
	b		58	-----	
	c		57	-----	
No.2-2	a	69	61	-----	
	b		59	-----	
	c		60	-----	
2-3	a	88	54	-----	
	b		54	-----	
	c		59	-----	
No.3	a	98	54	-----	
	b		54	-----	
	c		54	-----	

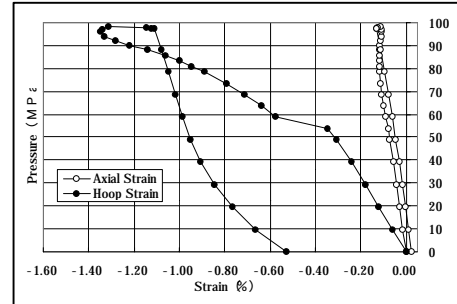


Fig.14 Test Result of PWR Cladding (98MPa)

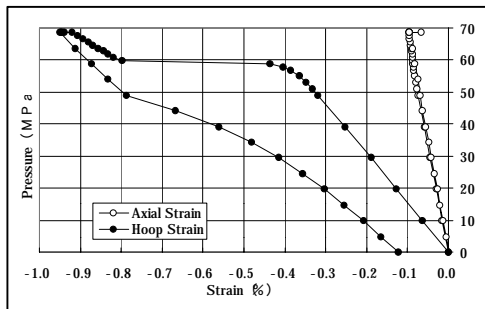


Fig.15 Test Result of PWR Cladding (69MPa)

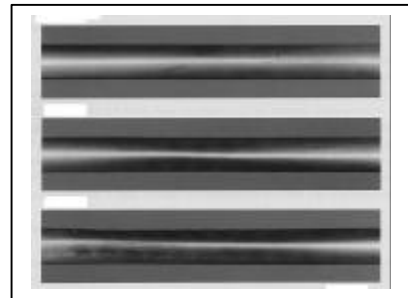


Photo.2 BWR Claddings after Buckling

Reference

- [1] Sprung, J.L., et al., Data and Methods for Assessment of the Risks Associated with the Maritime Transport of Radioactive Materials Results of the SeaRAM Program studies, SANDIA REPORT, SAND98-1171/1, 1998.
- [2] N.Watabe et al., An estimation method of marine accident probability for exclusive-use ships, Int. Journal of RAMTRANS, Vol.9, No.2,1998
- [3] Y.Gomi,et al., Demonstration Test for Transporting Vitrified High-Level Radioactive Waste : Water Immersion Test- Proc. of the 11th Int. Conf. On the PATRAM, Dec. 3-8, 1995